Check for updates

Journal of
Materials Chemistry C

Materials for optical, magnetic and electronic devices

rsc.li/materials-c

Volume 6
Number 5
7 February 2018
Pages 911-1266

ISSN 2050-7526

ROYAL SOCIETY OF CHEMISTRY

PAPER
Nosang V. Myung, Yong-Ho Choe et al.
A noble gas sensor platform: linear dense assemblies of single-walled carbon nanotubes (LACNTs) in a multi-layered ceramic/metal electrode system (MLES)

ROYAL SOCIETY OF CHEMISTRY

rsc.li/materials-c

ARTICLE

Role of Flexible Amide Spacers on the Self-assembly of Star-shaped Triphenylbenzenes with Photoactive Triphenylamine Units: Stimuli-responsive Liquid Crystals and Gels

Alejandro Martínez-Bueno,[a,b] Patricia Marín San Román,[a,b] Raquel Giménez*,[a,b] and Teresa Sierra*,[a,b]

This work reports on the decisive influence of the length of flexible amide spacers for obtaining soft materials out of star-shaped molecules. Either liquid crystal behaviour or gel behaviour was found for 1,3,5-triphenylbenzene connected to three triphenylamine units through flexible amide spacers with different number of carbon atoms. The spacer of two carbon atoms induces liquid crystal behaviour but not gel formation. Conversely, an analogous compound with three carbon atom spacer is not liquid crystalline and forms gels in different solvents. The obtained liquid crystal phase shows a hexagonal columnar organization responsive to electric fields, allowing the material to be aligned homeotropically in ITO cells, that is, with the columns perpendicular to the electrodes and parallel to the applied electric field. Taking advantage of the photoactivity of triarylamine units bearing amide groups, the response under light irradiation in gel state was explored.

Introduction

Liquid crystals (LCs) are archetypical examples of soft nanostructures in which conveniently tailored small molecules can yield functional assemblies able to respond to light, electric or magnetic fields.[1] Among the LC phases, the columnar mesophases hold great promise as new π-functional materials for organic electronic applications, as columns can act as a 1D nanostructure for anisotropic charge or ion transport,[2-4] or build a neat dipole moment to achieve new forms of soft polar nanostructures.[5]

Among molecular designs, not only discotic π-conjugated molecules, but less conventional ones such as three-arm star-shaped mesogens,[6] can give rise to columnar mesophases. Star-shaped molecules have attractive prospects, in part due to the synthetic versatility to introduce π-conjugated functional units at their arms,[7] either conjugated[8-15] or joined though a non-conjugated spacer.[16-21] Thus, columnar organizations with prominent semiconducting properties[10,22-26] or stimuli-responsive luminescence[8,27] have been reported.

To enhance the stability of these columnar architectures, hydrogen bond groups can be introduced in the arms to reinforce intermolecular/intracolumnar interactions. In this respect, aromatic tricarboxamides such as benzene-1,3,5-tricarboxamide (BTA) (Figure 1) are the most used star-shaped

structural motif to achieve hydrogen bonding stabilized columnar liquid crystals and/or nanoaggregates in solvents.[28]

The 1,3,5-benzene core has been also expanded to 1,3,5-triphenylbenzene (TPBs) (Figure 1), introducing additional levels of rotational mobility. In this respect, TPB trisamides have been studied for gels[29-30] and aggregates.[31] Concerning liquid crystal behaviour, several star-shaped mesogens with a TPB core have been described, albeit without amide groups,[32-37] finding an important interplay between molecular structures and modes of self-assembly.
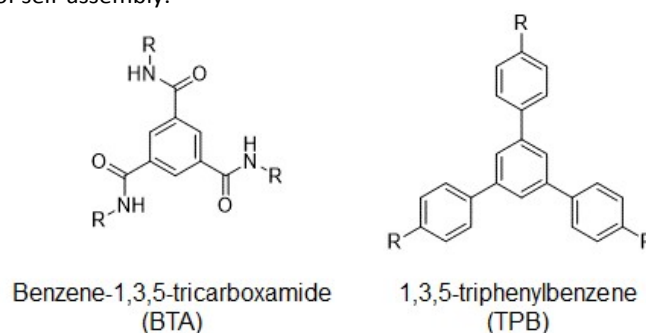

Figure1. Chemical structure of BTA and TPB star-shaped cores.

In this work, a novel design for star-shaped hydrogen bonded TPBs is reported, but unlike previously described BTA derivatives, the amide group is inserted within a short but flexible spacer of two or three carbon atoms (Scheme 1). This spacer is useful to bring higher flexibility, which in combination with hydrogen bonding abilities favours the formation of columnar phases stable at room temperature and gels.[17,22] Functional units derived from triphenylamine (TPA) have been introduced at the periphery to bring photoactive properties,

a. Instituto de Nanociencia y Materiales de Aragón (INMA), CSIC-Universidad de Zaragoza, 50009 Zaragoza, Spain.
b. Departamento de Química Orgánica, Facultad de Ciencias, Universidad de Zaragoza, 50009 Zaragoza, Spain.
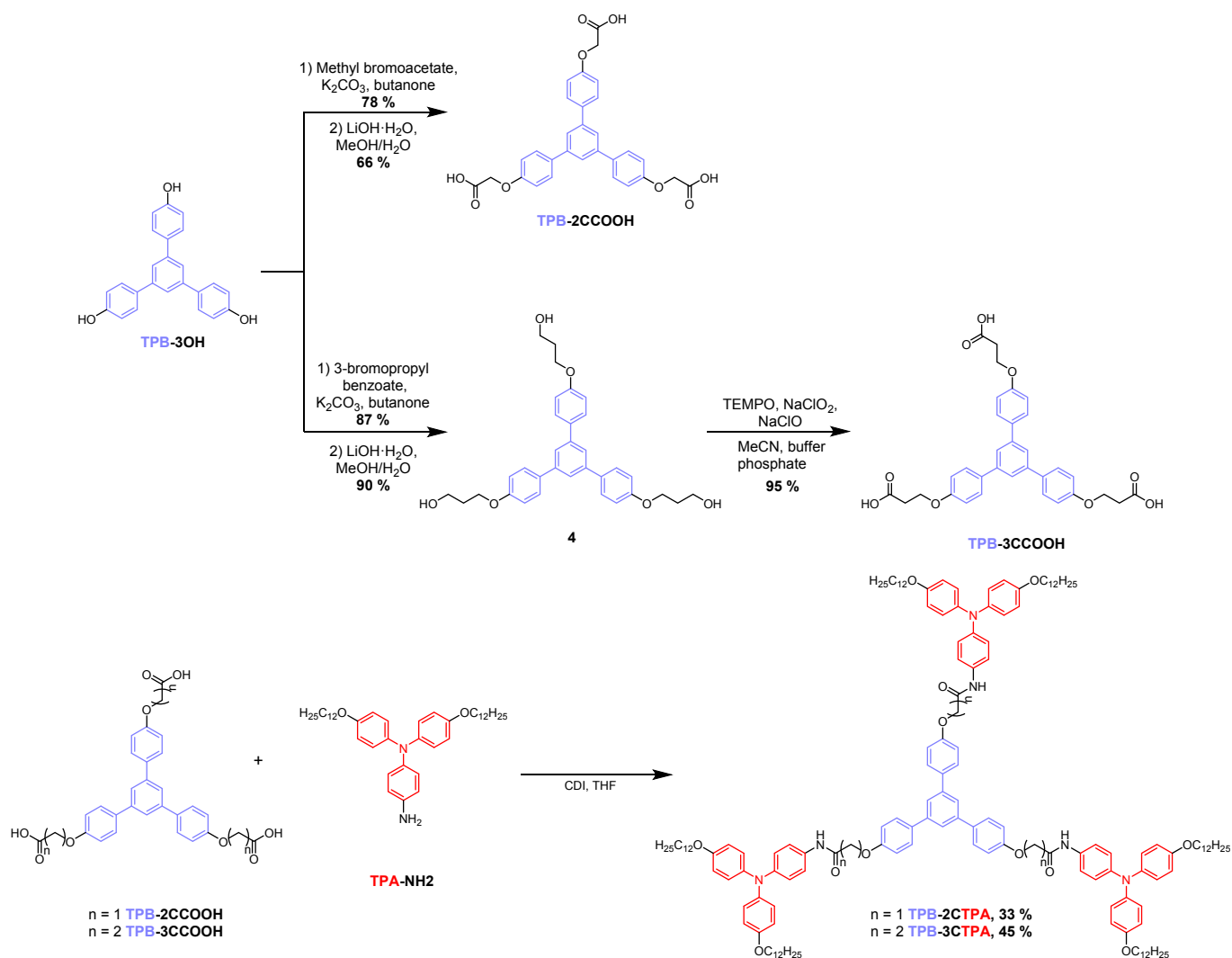
ARTICLE

leveraging the photooxidation behaviour of amide TPA derivatives.[38] In particular, we here describe the synthesis and properties of two TPB star-shaped molecules, namely **TPB-2CTPA** and **TPB-3CTPA**, their thermal properties, the contrast between hydrogen bonding patterns by IR spectroscopy, and their gel formation abilities. Different behaviour was found depending on the number of carbon atoms of the flexible amide spacers connecting the core with the arms. In addition, the presence of amide groups allowed to explore the response of the mesophase to electric fields and the photoactivity of TPA units in gel state.

Results and discussion

Synthesis

Star-shaped derivatives were synthesized as described in Scheme 1 and S1. Precursory compounds, **TPA-NH2**[22] and **TPB-3OH**[39] were prepared as reported previously. TPB with flexible spacers containing carboxylic acid moieties (**TPB-2CCOOH** and **TPB-3CCOOH**) were obtained from **TPB-3OH** via two different synthetic strategies. Compound **TPB-2CCOOH** was prepared by a Williamson etherification with methyl α-bromoacetate and subsequent hydrolysis of the esters to carboxylic acids. In the case of three-carbon length spacer precursor **TPB-3CCOOH**, the introduction of methyl β-bromopropionate through a Williamson etherification was not efficient due to an α,β-elimination side reaction occurring under these conditions. To avoid this, the etherification was carried out with 3-bromopropyl benzoate and after the deprotection of the terminal CH_2OH groups they were oxidized with (2,2,6,6-tetramethylpiperidin-1-yl)oxidanyl (TEMPO) and bleach to yield the carboxylic acids. The two final compounds were synthesized through a triple amidation reaction of the TPB-containing carboxylic acids (**TPB-2CCOOH** and **TPB-3CCOOH**) with **TPA-NH2** in the presence of 1,1′-Carbonyldiimidazole (CDI) as activating agent of the carboxylic acid.

Scheme 1. Synthetic procedure of TPA-triphenylbenzene derivatives.

ARTICLE

Liquid crystal and thermal properties

The thermal properties and the liquid crystal behaviour of **TPB-2CTPA** and **TPB-3CTPA** (Table 1) were studied by polarized optical microscopy (POM), differential scaning calorimetry (DSC), thermogravimetric analysis (TGA) and X-ray diffraction (XRD).

Upon cooling from the isotropic phase, POM observations of compound **TPB-2CTPA** revealed a birefringent fan-shaped texture (Figure 2a), characteristic of hexagonal columnar mesophases. This texture was fluid below the clearing temperature, and could be sheared, but became rigid at room temperature. This thermal behaviour agreed with the DSC thermogram of the first cooling cycle, which showed an exothermic peak at 94 ºC and a glass transition at 47 °C. The heating cycle was consistent with the cooling ones, showing a glass transition at 64 ºC and an endothermic peak with an onset at 100 °C, corresponding to the transition to the isotropic liquid (Figure 2b).

Table 1. Thermal properties and hexagonal lattice parameter.

Compound	Thermal properties[a] (T ºC, [ΔH kJ/mol])	$T_{5\%}$[b]	Lattice parameters
TPB-2CTPA	I 94 [2.2] Col_h 47 $Col_{h(g)}$ $Col_{h(g)}$ 64 Col_h 100 [3.0] I	363	a = 45.5 Å
TPB-3CTPA	I 115 [31.3] Cr Cr 127 [27.4] I	355	-

[a] Thermal data obtained from the first cooling process and the second heating process at a rate of 10 °C/min. Temperatures are taken at the onset. [b] Temperature corresponding to a 5% weight loss by thermogravimetry. $Col_{h(g)}$: glassy hexagonal columnar phase, Col_h: hexagonal columnar mesophase, I: isotropic liquid, Cr: crystalline phase.

The texture behaviour of **TPB-2CTPA** was also investigated under the application of an electric field given the possibility of attaining a net dipole moment along the column due to intermolecular hydrogen-bonded amide motifs.[16,40-43] For this purpose, the material was introduced in a commercial 5 µm ITO/glass cell. Upon cooling from the isotropic liquid, the columnar mesophase exhibited a birefringent fan-shaped texture (Figure 2c), with larger domains than the texture observed during previous POM studies. The application of a square-wave electric field (1.0 Hz, 20 Vpp) at 90 °C led to the darkening of the ITO area in 80 min, which is consistent with the evolution of the texture to a homeotropic alignment. This homeotropic texture is stable after removing the electric field and cooling at room temperature, while the ITO-free area retained the initial texture. The same effect was observed by applying a square-wave electric field (1.0 Hz, 50 Vpp) in the

isotropic liquid phase, followed by cooling under the applied field at a rate of 0.5 °C/min.

On the other hand, the analogue **TPB-3CTPA** with a longer spacer behave under the POM as a crystalline solid with an undefined texture. The corresponding thermogram shows only one thermal transition upon both heating and cooling, with an enthalpy value around 30 kJ/mol (Figure S4a). These results evidenced that this compound crystallizes directly from the isotropic liquid, without forming a mesophase, as confirmed by X-ray diffraction (XRD) experiments (Figure S4b).

The columnar mesomorphism of compound **TPB-2CTPA** was confirmed by XRD experiments performed at room temperature in samples cooled from the isotropic liquid (Figure 2d). The diffractogram shows three reflections in the small angle region related to distances with a ratio of d, $d/\sqrt{3}$ and $d/\sqrt{4}$, which correspond to the reflections (100), (110) and (200) of a hexagonal lattice with a lattice parameter a = 45.5 Å. Furthermore, a diffuse broad reflection is observed at 4.5 Å due to the molten nature of the alkyl chains, confirming the liquid crystalline behaviour. The absence of a maximum at high angles corresponding to an intermolecular distance along the column hinders the calculation of a stacking parameter (c), and therefore, impedes the correct estimation of the number of molecules per unit cell (Z). For similar star-shaped compounds with tris(triazolyl)triazine at the core, and a hexagonal columnar phase with parameters a = 49.5 Å, c = 3.4 Å and density = 1 g/cm^3, a Z = 2 value was considered.[22] Taking into account the similar molecular size and the lattice parameter obtained for **TPB-2CTPA** it is reasonable to propose a disordered columnar packing in which two molecules arrange on each column stratum on average (Figure 2e). The non-regular arrangement is in accordance with the fact that intracolumnar stacking is not observed and not all amide groups are involved in intermolecular hydrogen bonding interactions (see below).

Hydrogen bond studies by FTIR

The formation and strength of the intermolecular hydrogen bonds formed between amide groups in systems with C_3 symmetry and flexible amide spacers, which decouple the amide group from the star-shaped core, are strongly correlated with the spacer length.[17,22] To further investigate the differences in hydrogen bonding interactions among the amide groups in compounds **TPB-2CTPA** and **TPB-3CTPA**, and to correlate these differences with their respective spacer lengths and their final properties, variable-temperature FTIR studies were conducted.

At room temperature, the compound with the shortest spacer, **TPB-2CTPA**, exhibits two N–H stretching bands around 3300 and 3400 cm⁻¹ (Figure 3a), consistent with the presence of both

hydrogen-bonded and free N–H groups within the columnar assemblies, respectively. Additionally, the C=O stretching region appears as a broad band spanning 1650 to 1720 cm⁻¹, indicating an overlap of hydrogen-bonded and free C=O stretching vibrations. In contrast, **TPB-3CTPA** shows a single N–H stretching band centred at 3295 cm⁻¹ and a sharp C=O stretching band at 1660 cm⁻¹ (Figure 3b), suggesting that both the N–H and C=O groups are fully engaged in hydrogen bonds.

Upon heating **TPB-2CTPA**, the intensity of the associated amide N–H stretching band gradually decreased and shifted to higher wavenumbers, while the intensity of the free N–H stretching band increased. A similar trend was observed for the C=O stretching band, which shifted to higher wavenumbers as expected due to the progressive weakening of hydrogen bonds with increasing temperature.
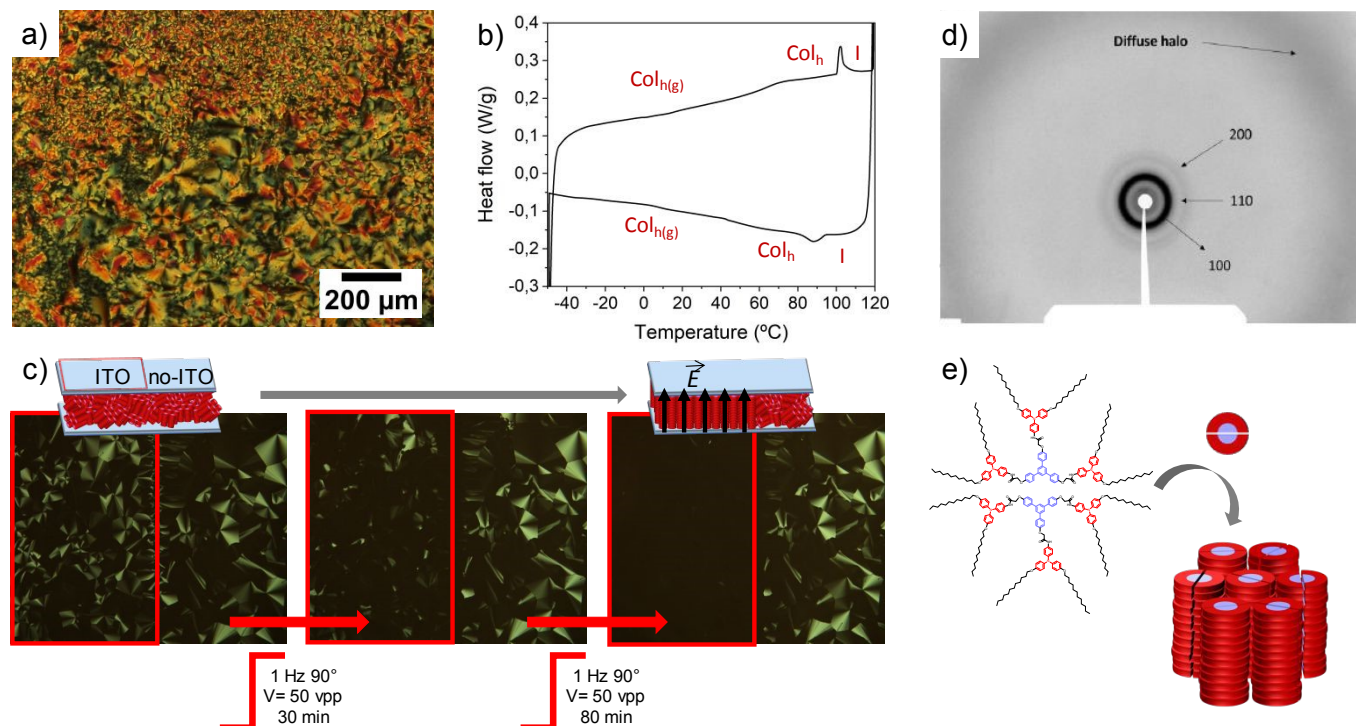

Figure 2. (a) Photomicrograph observed for compound **TPB-2CTPA** by POM at room temperature, (b) DSC thermogram of compound **TPB-2CTPA** corresponding to the first cooling process and the second heating process (c) photomicrographs observed for compound **TPB-2CTPA** by POM of the ITO/glass liquid crystal cell at different times after applying the *E*-field with a schematic representation of the process, (d) X-ray diffractogram of compound **TPB-2CTPA** at room temperature, and (e) Schematic representation of an idealized model for the self-assembly of **TPB-2CTPA** in the columnar liquid crystal phase.
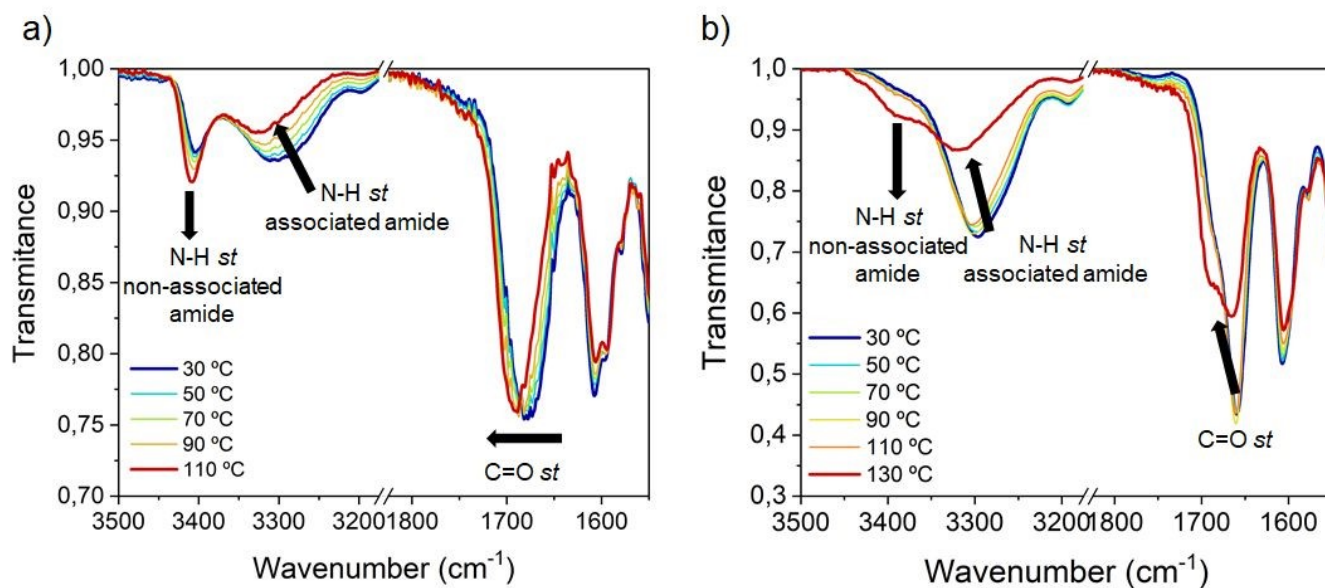

Figure 3. Infrared spectra of (a) **TPB-2CTPA** and (b) **TPB-3CTPA** at variable temperature.

ARTICLE

For **TPB-3CTPA**, no significant changes were observed in the associated N–H and C=O stretching bands until the transition to the isotropic liquid. At this temperature, both bands exhibited a marked intensity decrease along with an abrupt shift to higher wavenumbers. Additionally, the emergence of new bands at 3390 cm^{-1} and 1690 cm^{-1}, corresponding to free N–H and C=O stretching vibrations, respectively, indicated the partial disruption of intermolecular hydrogen bonds. This abrupt change at the melting temperature, is consistent with a crystalline phase.

These results revealed a clear distinction in the nature and strength of the intermolecular hydrogen bonding interactions of **TPB-2CTPA** and **TPB-3CTPA**, which correlates well with their different phase behaviour. For **TPB-2CTPA**, the presence of both hydrogen-bonded and free N–H and C=O stretching bands suggests the formation of more dynamic, ordered but fluid, hydrogen-bonded columnar aggregates. Also, this is consistent with a non-regular arrangement, as deduced from the absence of a reflection maximum at high angles in the DRX pattern related with a long-range stacking distance. In contrast, the longer and more flexible spacer in compound **TPB-3CTPA** facilitates hydrogen bonding interactions between amide groups, leading to enhanced stabilization of intermolecular interactions, thus favouring the formation of a crystalline phase.

Gel properties

As part of our ongoing efforts to identify versatile molecular platforms for the development of functional materials across different environments, including bulk and solution,[44] we further explored the ability of these two molecules to act as building blocks for soft self-assembled materials formed in different solvents at a concentration on 1 wt% (Table S1). Notably, compound **TPB-3CTPA** formed opaque gels in 1-octanol (Figure 4a), semi-transparent gels in dodecane (Figure 4b) and transparent gels in toluene (Figure 4c). However, compound **TPB-2CTPA** is soluble in all of these solvents at this concentration. These results support the critical role of the spacer length in the self-assembly ability of these compounds, as already observed in their liquid crystalline behaviour.
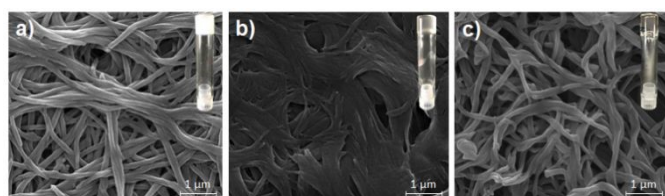

Figure 4. SEM images of xerogels of compound **TPB-3CTPA** (a) from 1-octanol, (b) from dodecane and (c) from toluene

The morphology of the aggregates formed by **TPB-3CTPA** in each solvent was analysed by scanning electron microscopy (SEM) of the xerogels. All the three xerogels show a fibrillar morphology, regardless of the solvent employed. 1-octanol xerogel displayed entangled fibril bundles with an average width of 150 nm (Figure 4a). In the case of dodecane xerogel, larger aggrupation of fibres made of smaller fibres of 75 nm on average width can be distinguished (Figure 4b). The xerogel in toluene displays fibril bundles with a width of 100 nm on average (Figure 4c).

Some TPA derivatives containing at least one amide group,[36,45-50] or a carboxylic group[51] have the ability to generate radical cation species under light irradiation in the presence of chlorinated solvents (Figure 5a). In this respect, the photoresponse of **TPB-3CTPA** was investigated both in dilute dichloromethane solution, and in the 1-octanol gel by introducing a small amount of dichloromethane (DCM). These studies were carried out using UV-vis (Figure 5b, d) and ^{1}H NMR spectroscopy (Figure 5c).

The solution was initially colourless, and the UV-vis spectrum exhibited two intense absorption bands at 275 nm and 310 nm, along with two weaker bands at 405 nm and 800 nm (Figure 5b, black line). After 2 minutes of irradiation with a Hg lamp, the solution turned light green, and the bands at 275 nm, 405 nm and 800 nm showed a marked intensity increase, except for the 310 nm band, which displayed a pronounced decrease. In addition, three new absorption bands appeared at 725 nm, 650 nm, and 465 nm (Figure 5b, green line). These spectral changes are attributed to the formation of the triarylammonium radical cation, which was also observed to form by cyclic voltamperometry (Figure S5), and it is known to exhibit a strong absorption in the near-infrared region.[38,52] After 16 minutes of irradiation, the solution turned orange, and the absorption bands at 800 nm, 725 nm, and 650 nm almost disappeared, while the band at 465 nm increased in intensity (Figure 5b, orange line). The orange color is consistent with the formation of the dicationic species, which has been reported to absorb in the visible range and represents a further oxidation state of the TPA moieties.[52]

In the case of the ^{1}H NMR spectra, the initial spectrum displayed well-resolved signals corresponding to the aromatic protons of the TPA moieties, the TPB core, the spacer, and the aliphatic chains (Figure 5c). After irradiation, all signals attributable to the TPA protons vanished, while the signals corresponding to the TPB aromatic core and the aliphatic chains remained observable. This behaviour is consistent with previously reported photoinduced aggregation and radical formation processes involving TPA derivatives in chlorinated solvents, in which the disappearance of proton signals has been attributed

ARTICLE

to the formation of the triarylammonium radicals and subsequent supramolecular self-assembly into highly anisotropic aggregates.[38,52-53]

The modification of the gelation properties through the photooxidation process was studied for the 1-octanol gel by introducing 5 wt% of dichloromethane. As in the case of the solution, short irradiation times induced the generation of light green colour in the gel due to the presence of the triarylammonium radical cations as confirmed in the UV-vis spectrum (Figure 5d). As observed for the solution, longer

irradiation times produced the formation of dicationic species and resulted in the disruption of the gel. This phenomenon is attributed to the increased charge density and stronger electrostatic repulsion between the dicationic units, which interferes with the non-covalent interactions, such as π–stacking or van der Waals forces, responsible for maintaining the integrity of the supramolecular network.

Finally, the photooxidation process did not occur in a solution of the compound in acetone or in the gel in 1-octanol, that is, in absence of chlorinated solvents.
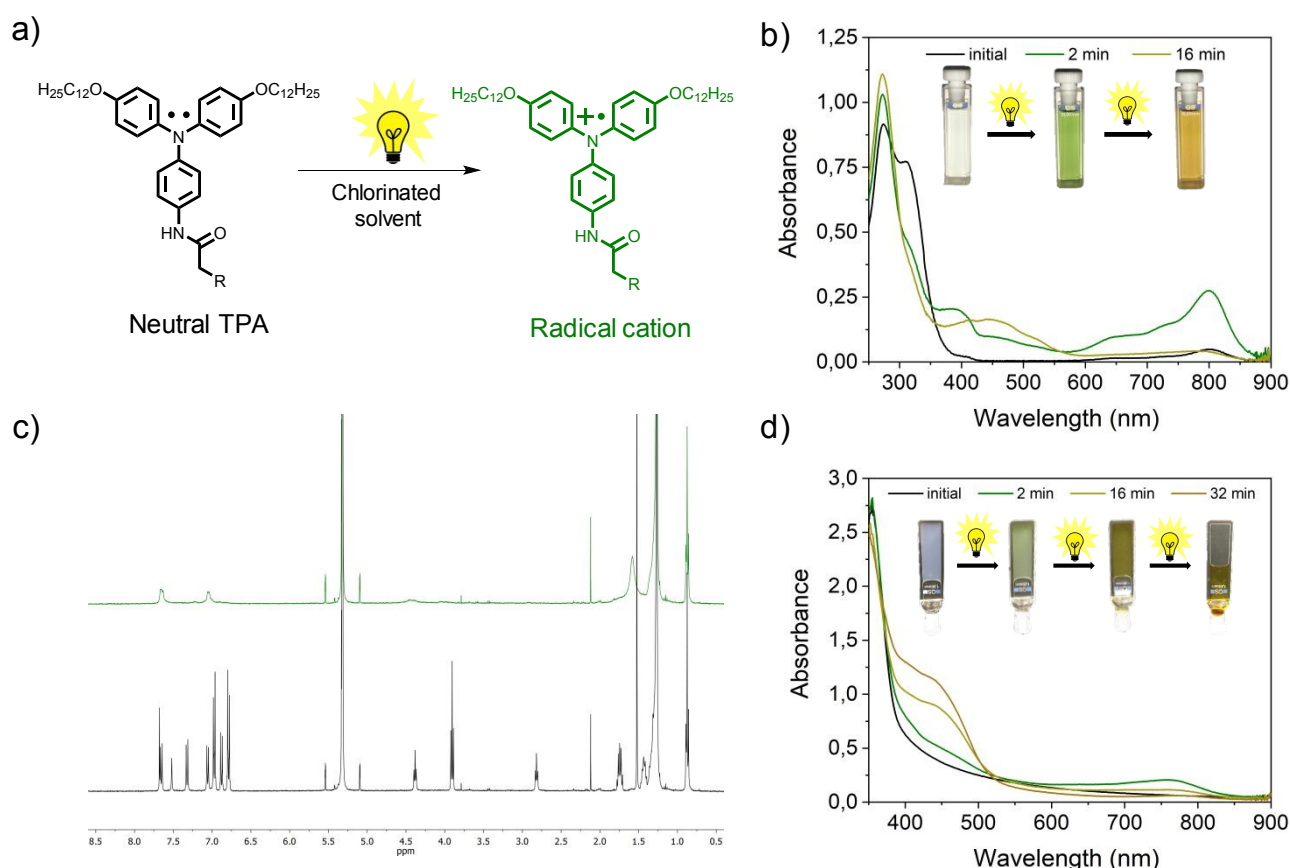

Figure 5. (a) Schematic representation of TPA oxidation in presence of chlorinated solvents. (b) UV-vis spectra recorded for **TPB-3CTPA** in dichloromethane solution (10^{-5} M) at different times of irradiation and the respective pictures of the sample. (c) ^{1}H NMR spectra recorded for **TPB-3CTPA** in deuterated dichloromethane solution (2.5·10^{-3} M) before (down) and after irradiating the solution during 1 min (up). (d) UV-vis spectra recorded for **TPB-3CTPA** gel at 1 wt% in 1-octanol/dichloromethane (95/5) (10^{-5} M) at different times of irradiation and the respective pictures of the sample.

Conclusions

The contrasting behaviour of two derivatives of TPB differing only in the length of the flexible amide spacer is demonstrated. Whereas the compound with a two-carbon atom spacer yields liquid crystalline behaviour, whose order can be maintained in a glassy state at room temperature and can be oriented under electric fields, the compound with a three-atom carbon spacer is crystalline. FTIR experiments confirm differences in the stablishment of intermolecular hydrogen bonding interactions between amide groups that align with the differences observed in phase behaviour. Indeed, the compound with a three-carbon spacer shows a full engagement of amide groups in hydrogen

bonding interactions in contrast to the two-carbon spacer compound, which shows partial formation of hydrogen bonds. Furthermore, the formation of aggregates in solvents is also different depending on the spacer length, and only the three-carbon spacer derivative can yield organogels in different solvents at 1 wt %. It is demonstrated that the TPA redox unit photooxidizes in the gel state under light irradiation by adding a small amount of a chlorinated solvent, which is interesting for stimuli-responsive gels and optoelectronic applications.

Author contributions

A.M.-B.: investigation, methodology, data curation, writing – original draft. P. M. S. R.: investigation, methodology, data curation. R.G.: conceptualization, formal analysis, validation, supervision, funding

acquisition, writing – review & editing. T.S.: conceptualization, formal analysis, validation, supervision, funding acquisition, writing – review & editing.

Conflicts of interest

There are no conflicts to declare.

Data availability

The data supporting this article have been included as part of the Supplementary Information.

Acknowledgements

Notes and references

1 H. K. Bisoyi and Q. Li, *Chem. Rev.*, 2022, **122**, 4887.
2 T. Wöhrle, I. Wurzbach, J. Kirres, A. Kostidou, N. Kapernaum, J. Litterscheidt, J. C. Haenle, P. Staffeld, A. Baro, F. Giesselmann and S. Laschat, *Chem. Rev.*, 2016, **116**, 1139.
3 T. Kato, M. Yoshio, T. Ichikawa, B. Soberats, H. Ohno and M. Funahashi, *Nature Rev. Mater.*, 2017, **2**, 17001.
4 R. De and S. K. Pal, *Chem. Commun.*, 2023, **59**, 3050.
5 T. M. Swager, *Acc. Chem. Res.*, 2022, **55**, 3010.
6 M. Lehmann, in Handbook of Liquid Crystals, Eds: J. W. Goodby, P. J. Collings, T. Kato, C. Tschierske, H. Gleeson, P. Raynes, P., Wiley-VCH: Weinheim, 2014; Vol. 5, 2nd ed.
7 H. M. Diab, A. M. Abdelmoniem, M. R. Shaaban, I. A. Abdelhamid and A. H. M. Elwahy, *RSC Adv.*, 2019, **9**, 16606.
8 C.-Y. Zeng, W.-J. Deng, K.-Q. Zhao, C. Redshaw, B. Donnio, *Chem. Eur. J.* 2024, **30**, e202400296.
9 I. Bala, H. Kaur, M. Maity, R. A. K. Yadav, J. De, S. P. Gupta, J.-H. Jou, U. K. Pandey and S. K. Pal, *ACS Appl. Electron. Mater.*, 2022, **4**, 1163.
10 S. Dhingra, I. Bala, J. De, S. P. Gupta, U. K. Pandey, S. K. Pal, *J. Mater. Chem. C* 2021, **9**, 5628.
11 N. Tober, T. Rieth, M. Lehmann and H. Detert, *Chem.-Eur. J.*, 2019, **25**, 15295.
12 F. A. Olate, M. L. Parra, J. M. Vergara, J. Barberá and M. Dahrouch, *Liq. Cryst.*, 2017, **44**, 1173.
13 S. K. Pathak, S. Nath, J. De, S. K. Pal, A. S. Achalkumar, *New J. Chem.* 2017, **41**, 9908.
14 H. Detert, M. Lehmann and H. Meier, *Materials*, 2010, **3**, 3218.
15 R. Cristiano, J. Eccher, I. H. Bechtold, C. N. Tironi, A. A. Vieira, F. Molin, H. Gallardo, *Langmuir* 2012, **28**, 11590.
16 J. Bi, J. Uchida, T. Kato, *New J. Chem.* 2025, **49**, 3708.
17 A. Martínez-Bueno, R. Vidal, J. Ortega, J. Etxebarria, C. L. Folcia, R. Giménez and T. Sierra, *Mater. Today Chem.* 2023, **29**, 101394.
18 E. Beltran, M. Garzoni, B. Feringan, A. Vancheri, J. Barbera, J. L. Serrano, G. M. Pavan, R. Gimenez and T. Sierra, *Chem. Commun.*, 2015, **51**, 1811.
19 K.-Q. Zhao, X.-Y. Bai, B. Xiao, Y. Gao, P. Hu, B.-Q. Wang, Q.-D. Zeng, C. Wang, B. Heinrich and B. Donnio, *J. Mater. Chem. C*, 2015, **3**, 11735.
20 I. Paraschiv, M. Giesbers, B. van Lagen, F. C. Grozema, R. D. Abellon, L. D. A. Siebbeles, A. T. M. Marcelis, H. Zuilhof, E. J. R. Sudhölter, *Chem. Mater.* 2006, **18**, 968.
21 C. P. Umesh, A. T. M. Marcelis, H. Zuilhof, *Liq. Cryst.* 2015, **42**, 1269.
22 A. Martínez-Bueno, S. Martín, J. Ortega, C. L. Folcia, R. Termine, A. Golemme, R. Giménez and T. Sierra, *Chem. Mater.*, 2024, **36**, 4343.
23 S. Gómez-Esteban, A. Benito-Hernandez, R. Termine, G. Hennrich, J. T. L. Navarrete, M. C. Ruiz-Delgado, A. Golemme, B. Gómez-Lor, *Chem. Eur. J.* 2018, **24**, 3576.
24 A. Benito-Hernández, U. K. Pandey, E. Cavero, R. Termine, E. M. García-Frutos, J. L. Serrano, A. Golemme, B. Gómez-Lor, *Chem. Mater.* 2013, **25**, 117.
25 T. Yasuda, T. Shimizu, F. Liu, G. Ungar, T. Kato, *J. Am. Chem. Soc.* 2011, **133**, 13437.
26 Paraschiv, K. de Lange, M. Giesbers, B. van Lagen, F. C. Grozema, R. D. Abellon, L. D. A. Siebbeles, E. J. R. Sudholter, H. Zuilhof and A. T. M. Marcelis, *J. Mater. Chem.*, 2008, **18**, 5475.
27 R. K. Gupta, S. K. Pathak, J. De, S. K. Pal and A. S. Achalkumar, *J. Mater. Chem. C*, 2018, **6**, 1844.
28 S. Cantekin, T. F. A. de Greef and A. R. A. Palmans, *Chem. Soc. Rev.*, 2012, **41**, 6125.
29 Y. He, Z. Bian, C. Kang, Y. Cheng and L. Gao, *Tetrahedron*, 2010, **66**, 3553.
30 H.-K. Yang, H. Zhao, P.-R. Yang and C.-H. Huang, *Colloids Surf, A* 2017, **535**, 242.
31 S. Díaz-Cabrera, Y. Dorca, J. Calbo, J. Aragó, R. Gómez, E. Ortí and L. Sánchez, *Chem. Eur. J.* 2018, **24**, 2826.
32 Y.-F. Bai, W. Li-Qin, H. Ping, L. Kai-Jun, Y. Wen-Hao, N. Hai-Liang, Z. Ke-Qing and B.-Q. and Wang, *Liq. Cryst.*, 2015, **42**, 1591.
33 T. Wöhrle, H. Taing, C. Schilling, S. H. Eichhorn and S. Laschat, *Liq. Cryst.*, 2019, **46**, 1973.
34 Obsiye, T. Wöhrle, J. C. Haenle, A. Bühlmeyer and S. Laschat, *Liq. Cryst.* 2018, **45**, 164.
35 T. Wohrle, S. J. Beardsworth, C. Schilling, A. Baro, F. Giesselmann and S. Laschat, *Soft Matter*, 2016, **12**, 3730-3736.
36 K. Bader, T. Wöhrle, E. Öztürk, A. Baro, S. Laschat, *Soft Matter* 2018, **14**, 6409.
37 M. A. Grunwald, T. Wöhrle, R. Forschner, A. Baro, S. Laschat, *Eur. J. Org. Chem.* 2020, **2020**, 2190.
38 E. Moulin, F. Niess, M. Maaloum, E. Buhler, I. Nyrkova and N. Giuseppone, *Angew. Chem. Int. Ed.*, 2010, **49**, 6974-6978.
39 B. P. Dash, R. Satapathy, J. A. Maguire and N. S. Hosmane, *Organometallics*, 2010, **29**, 5230.
40 C. F. C. Fitie, W. S. C. Roelofs, M. Kemerink and R. P. Sijbesma, *J. Am. Chem. Soc.*, 2010, **132**, 6892.
41 K. Sato, Y. Itoh and T. Aida, *J. Am. Chem. Soc.*, 2011, **133**, 13767.
42 D. Miyajima, F. Araoka, H. Takezoe, J. Kim, K. Kato, M. Takata and T. Aida, *Angew. Chem. Int. Ed.*, 2011, **50**, 7865.
43 J. Guilleme, E. Cavero, T. Sierra, J. Ortega, C. L. Folcia, J. Etxebarria, T. Torres and D. González-Rodríguez, *Adv. Mater.*, 2015, **27**, 4280.

Journal of Materials Chemistry C Accepted Manuscript

44 M. Castillo-Vallés, A. Martínez-Bueno, R. Giménez, T. Sierra, M. B. Ros, *J. Mater. Chem. C* 2019, **7**, 14454.

45 E. Moulin, E. Busseron, Y. Domoto, T. Ellis, A. Osypenko, M. Maaloum, N. Giuseppone, *Comptes Rendus Chim.* 2016, **19**, 117.

46 Y. Domoto, E. Busseron, M. Maaloum, E. Moulin, N. Giuseppone, *Chem. Eur. J.* 2015, **21**, 1938.

47 E. Busseron, J. J. Cid, A. Wolf, G. Du, E. Moulin, G. Fuks, M. Maaloum, P. Polavarapu, A. Ruff, A. K. Saur, S. Ludwigs, N. Giuseppone, *ACS Nano* 2015, **9**, 2760.

48 J. Kim, J. Lee, W. Y. Kim, H. Kim, S. Lee, H. C. Lee, Y. S. Lee, M. Seo, S. Y. Kim, *Nat. Commun.* 2015, **6**, 6959.

49 R. J. Kumar, Q. I. Churches, J. Subbiah, A. Gupta, A. Ali, R. A. Evans, R. A. Holmes, *Chem. Commun.* 2013, **49**, 6552

50 E. Moulin, F. Niess, G. Fuks, N. Jouault, E. Buhler, N. Giuseppone, *Nanoscale* 2012, **4**, 6748.

51 B. Feringán, A. Martínez-Bueno, T. Sierra and R. Giménez, *Molecules*, 2023, **28**, 2887.

52 T. K. Ellis, M. Galerne, J. J. Armao IV, A. Osypenko, D. Martel, M. Maaloum, G. Fuks, O. Gavat, E. Moulin and N. Giuseppone, *Angew. Chem. Int. Ed.*, 2018, **57**, 15749.

53 I. Nyrkova, E. Moulin, J. J. Armao, M. Maaloum, B. Heinrich, M. Rawiso, F. Niess, J. J. Cid, N. Jouault, E. Buhler, A. N. Semenov and N. Giuseppone, *ACS Nano*, 2014, **8**, 10111.